Chemosphere 91 (2013) 35–40

Contents lists available at SciVerse ScienceDirect

Chemosphere

journal homepage: www.elsevier.com/locate/chemosphere

Chemical and structural analysis of enhanced biochars: Thermally treated mixtures of biochar, chicken litter, clay and minerals

Y. Lin [a], P. Munroe [a,*], S. Joseph [a], A. Ziolkowski [b], L. van Zwieten [c], S. Kimber [c], J. Rust [c]

[a] School of Materials Science and Engineering, The University of New South Wales, Sydney, NSW 2052, Australia
[b] School of Environmental and Life Sciences, The University of Newcastle, NSW 2258, Australia
[c] Wollongbar Primary Industries Institute, 1243 Bruxner Highway, Wollongbar, NSW 2477, Australia

HIGHLIGHTS

- ▶ Enhanced biochars were prepared based on torrefaction of biochar and mineral phases.
- ▶ Torrefaction was effective in minimising nitrogen losses from feedstocks.
- ▶ Higher processing temperatures promoted enhanced dissolved organic carbon content.

ARTICLE INFO

Article history:
Received 24 August 2012
Received in revised form 21 November 2012
Accepted 23 November 2012
Available online 25 December 2012

Keywords:
Biochar
LC-OCD
Dissolved organic carbon
Chicken litter

ABSTRACT

In this study biochar mixtures comprising a Jarrah-based biochar, chicken litter (CL), clay and other minerals were thermally treated, via torrefaction, at moderate temperatures (180 and 220 °C). The objectives of this treatment were to reduce N losses from CL during processing and to determine the effect of both the type of added clay and the torrefaction temperature on the structural and chemical properties of the final product, termed as an enhanced biochar (EB). Detailed characterisation indicated that the EBs contained high concentrations of plant available nutrients. Both the nutrient content and plant availability were affected by torrefaction temperature. The higher temperature (220 °C) promoted the greater decomposition of organic matter in the CL and dissociated labile carbon from the Jarrah-based biochar, which produced a higher concentration of dissolved organic carbon (DOC). This DOC may assist to solubilise mineral P, and may also react with both clay and minerals to block active sites for P adsorption. This subsequently resulted in higher concentrations of plant available P. Nitrogen loss was minimised, with up to 73% of the initial total N contained in the feedstock remaining in the final EB. However, N availability was affected by both torrefaction temperature and the nature of the clay minerals added.

© 2012 Elsevier Ltd. All rights reserved.

1. Introduction

The poultry industry generates large volumes of chicken litter (CL). This is rich in plant nutrients, such as nitrogen and phosphorus, consequently CL has for some decades been applied to agricultural soils as an organic ffertilizer (Faridullah et al., 2008). However, direct land application of untreated CL to soil has many disadvantages, such as the environmental pollution caused by pathogens, ammonia emission, nitrate contamination of groundwater (Nahm, 2003), and soluble P contamination of surface water, especially when CL is overapplied (Faridullah et al., 2008). Composting CL with biomass, such as straw and sawdust, is increasingly considered to be an effective method for recycling surplus manure as a stabilised and sanitised end product, since this process can eliminate pathogens and weeds, reduces both volume and moisture and can generate higher quality fertilizers (Bernal et al., 2009). However, it was found (Ogunwande et al., 2008) that cumulative N loss was up to 71% of the initial total N under optimal conditions during composting, mainly due to volatilisation of ammonia. Nitrogen loss decreased both the fertilizer potential and economic value of the end product, while causing environmental pollution (Kithome et al., 1999; Bernal et al., 2009; Steiner et al., 2010).

To reduce N loss and optimise the C/N ratio, biochar, as a bulking agent, has been used in the composting process (Steiner et al., 2010; Clough and Condron, 2010; Jindo et al., 2012). The total N losses were decreased to ~40% (Steiner et al., 2010). However, composting is not always the optimum strategy to recycle organic material produced by animals. Further, this approach is still not widely accepted as a commercially viable process because the composting process is relatively time consuming (Shinogi et al., 2003; Jindo et al., 2012).

---

* Corresponding author.
E-mail address: p.munroe@unsw.edu.au (P. Munroe).

0045-6535/$ - see front matter © 2012 Elsevier Ltd. All rights reserved.
http://dx.doi.org/10.1016/j.chemosphere.2012.11.063

By combustion or pyrolysis of CL, the stabilized product, that is a CL biochar and ash mixture, can be used as fertilizer with fewer adverse effects (Faridullah et al., 2008). However, significant nitrogen loses during this thermal treatment makes the CL-based biochar less effective as a nitrogen resource (Steiner et al., 2010). Pyrolysis of CL at temperatures of 400 and 500 °C resulted in N losses as high as 69% and 76%, respectively (Gaskin et al., 2008). In addition, it has been reported (Cao and Harris, 2010) that higher temperature (e.g. 500 °C) treatment may decrease the water soluble P content in biochars, in this case from dairy manure feedstocks, due to crystallization of calcium phosphate as a thermodynamically stable phase.

On the other hand, biochar amendment to increase soil fertility and crop yield has attracted significant interest over the past decade. It has been reported that biochar application can reduce soil acidity (Shinogi et al., 2003), and increase soil cation exchange capacity (CEC) (Liang et al., 2006) and nutrient retention (Glaser et al., 2002). Taghizadeh-Toosi (2011) found that in the presence of biochar, ammonia and nitrous oxide (N_2O) emissions from soils under ruminant urine patches were reduced due to NH_3 uptake by the biochar. Moreover, ammonia adsorbed by biochar was stable, but readily plant available, when applied to soils.

Anthroterra Pty. has developed a patented process (PCTI/AU2010/000534) to produce a biochar–mineral mixture, that combined the benefits of biochar, that is, a high content of nutrients with those of a sterilised organic amendment (Lin et al., 2012a). Such materials are produced by mixing wood biochar with CL, clay and minerals, and torrefying the mixture at moderate temperature (220 °C). It has been confirmed that clay and minerals become incorporated into the biochar to form biochar–mineral-complexes where a high concentration of dissolved organic carbon (DOC) is present (Lin et al., 2012a). The microstructure generated is similar to that observed in Terra Preta particles (Chia et al., 2012).

Torrefaction of the biochar mixed with CL, clay and minerals is likely to produce a nutrient-rich biochar mixture, termed here as an enhanced biochar (EB), but nutrient conservation and availability in these materials has not been investigated. The role of DOC and the effect of clay and torrefaction temperature on EBs are unclear. Thus, the objective of this study was to determine the effect of clay type and torrefaction temperature on the structural and chemical characteristics of EBs for agricultural use. Specifically, one goal was to compare characteristics critical for agricultural use including pH, CEC, total nutrient concentrations, and potentially available nutrient concentrations in the EBs from two kinds of clay and two processing temperatures.

2. Materials and methods

A biochar (termed here SIM) was produced from Jarrah sawdust in a vertical retort at a temperature of approximately 600 °C with a processing time of 24 h. The biochar was then treated with a 1 M phosphoric acid solution. This treatment was carried out at 90 °C for 1 h, and then the mixture was cooled down to room temperature and held there for 24 h. CL (results from proximate and ultimate analysis are listed in Table 1), clay and minerals were added into the pretreated biochar slurry and mixed. Approximately 30% (dry weight) of the mixture was biochar, 30% chicken manure, 30% kaolinitic clay and the remainder a mixture of rock phosphate, basalt dust, calcium carbonate, and illemnite. The nature of the mineral phases added was based on the phases observed in Terra Preta particles (Chia et al., 2012). After drying the mixture at 80 °C for 24 h and the mixture was torrefied at an elevated temperature of either 180 or 220 °C for 4 h and cooled to room temperature. Three EBs were produced:

EB-1 and EB-2: contained a clay phase, termed Clay-1, sourced from a local brickworks, the biochar mixture was torrefied at either 180 (EB-1) or 220 °C (EB-2), respectively.

EB-3: contained a clay phase, termed Clay-2, which is a coal tailings material (from Newcastle, NSW, Australia), torrefaction was performed at 220 °C.

Table 1
The proximate and ultimate analysis results for all feedstocks used.

	Chicken litter	SIM biochar	Clay-1	Clay-2
Proximate analysis (%)				
Moisture	11.4	1.0	4.2	2.1
Ash	25.4	7.8	86.8	34.8
Volatile Matter	57.8	16.2	9.0	28.2
Fixed carbon	5.4	75.0	0.0	34.9
Ultimate analysis of feed stocks (% dry basis)				
Carbon	33.6	76.1	3.3	50.5
Hydrogen	4.2	1.8	0.2	4.1
Nitrogen	5.6	0.4	0.1	1.3
Total sulphur	0.5	<0.1	<0.1	0.8
Oxygen	27.4	14.4	5.8	7.7
Ash	28.7	7.2	90.6	35.5

The results of proximate and ultimate analysis for all feedstocks, including Clay-1 and Clay-2, are listed in Table 1. X-ray diffraction (XRD) was used to identify the mineral phases in both clays. Results are listed in Table 2. XRD was performed using a PANAnalytical X'Pert Pro PW3040 diffractometer using Cu Kα radiation with a wavelength of 0.15406 nm. Mineral identification was undertaken using the X'Pert High Score Plus search/match software. Rietveld quantitative analysis was performed on the XRD data by using a commercial package, SIROQUANT V3, from Sietronics Pty. The mineral phase abundances were estimated as relative abundances of the overall crystalline portion. Any amorphous material present was not quantified.

For direct observation of the interface between biochar and minerals within EB particles, the samples were embedded in epoxy resin, and mirror-polished to produce cross-sections of the particles. The polished samples were coated either with Cr for scanning electron microscope (SEM) observation and analysis (Hitachi 3400N SEM, to which energy dispersive X-ray spectroscopy facilities (EDS) were attached) or with Au for preparation of electron transparent sections, via a focused ion beam microscope, using methods described elsewhere (Munroe, 2009). These thin sections were examined using a transmission electron microscope (TEM) (Philips CM200 field emission TEM).

To analyse the bonding state for both carbon and nitrogen, the EBs were analysed using X-ray photoelectron spectroscopy (XPS) (VG ESCALAB-220i-XL) with a monochromatic Al Kα X-ray source ($h\nu = 1486.6$ eV) induced by 10 kV, 15 mA Al Kα radiation with a spot size ~1 mm in diameter. The pass energy for region scans was 20 eV with a scan step of 0.1 eV. The peak fitting program, Eclipse 2.0, was used to deconvolute the C 1s peak and the N 1s peak.

The EBs underwent a water extraction procedure to prepare specimens for DOC measurement by liquid chromatography - organic carbon detection (LC-OCD) technique. 10 g of the sample material was added to 100 mL of distilled water at 50 °C and held for 24 h. The mixture was centrifuged, and then filtered to separate the solid and liquid phases. The supernatants were passed through 0.45 µm filter and analysed (2 replicates were used) by a LC-OCD Model 8 (DOC-Labor, Eisenbahnstrasse 6, D-76229 Karlsruhe, Germany). Details of the measurement procedure have been described elsewhere in full by Huber et al. (2011). In this study, a phosphate buffer mobile phase of pH 6.4 ($2.6\ \mathrm{g\ L^{-1}}$ KH_2PO_4 and $1.5\ \mathrm{g\ L^{-1}}$ Na_2HPO_4) at a flow rate of $1.1\ \mathrm{mL\ min^{-1}}$ was applied. Injection

Table 2
Mineral crystal phases identified by XRD and the crystal phase quantitative results of Clay-1 and Clay-2 (relative dry weight, %).

Clay-1	Mineral composition	wt%	Clay-2	Mineral composition	wt%
			Mixed layer clay	Silicate	11
Kaolinite	$Al_2Si_2O_5(OH)_4$	34.4	Kaolinite	$Al_2Si_2O_5(OH)_4$	42
Quartz	SiO_2	33.7	Quartz	SiO_2	15
Muscovite	$K_{0.8}Na_{0.2}Fe_{0.05}Al_{2.95}Si_{3.01}O_{10}(OH)_2$	30.8	Muscovite/illite	Silicate	23
Anatase	TiO_2	0.7	Calcite	$CaCO_3$	3
Rutile	TiO_2	0.7	Ankerite	$Ca(Fe,Mg)(CO_3)_2$	3
Hematite	Fe_2O_3	0.2	Analcite	$NaAlSi_2O_6{\cdot}H_2O$	2
			Pyrite	FeS_2	1
Total		100	Total		100

volumes were 1000 μL. The chromatography subdivides DOC into six sub-fractions, which are assigned to specific classes of compounds: specifically, biopolymers, humics, building blocks, low molecular-weight acids, low molecular-weight neutrals and hydrophobic organic carbon (Huber et al., 2011). Their definitions can be found described in detail by others (Huber et al., 2011; Lin et al., 2012a,b).

The analysis of the EB properties (pH, total nitrogen, total carbon, CEC, acid-neutralising capacity (ANC), exchangeable cations, plant available phosphorus and extractable NH_4^+ and NO_3^- content) was performed by the New South Wales Industry and Investment using methods described by van Zweiten et al. (2010).

3. Results and discussion

SEM observation was carried out on the EB particles. Cross-sectional backscattered electron images from the polished cross-sections of the EBs revealed a similar microstructure from all three EBs. Representative images of EB-1 are shown in Fig. 1. Most of the biochar particles were, at least partially, surrounded by mineral phases. Further, some of pores within the biochar particles were evidently filled with mineral phases. However, most of the pores visible were free of minerals. This indicated some incorporation of the mineral phases within the biochar occurred during mixing and torrefaction, but the mineral phases preferentially located at the external surface of the particles, consistent with earlier studies reported by Lin et al. (2012a), although in this study a higher pyrolysis temperature biochar (~600 °C) and a different source of clays were used. The interaction of biochar and minerals is presumably due to chemical reactions that occurred on the biochar surface, for example, where biochar carboxylic groups have reacted with cations and positively charged Al oxides or oxyhydroxides (Joseph et al., 2010). No significant differences were noted between the three EBs studied.

Cross-sectional SEM EDS elemental maps of an EB-1 particle (Fig. SM-1 in Supplemental Material (SM)) showed that an Al-rich phase, presumably alumina-based, was located directly adjacent to a C-rich phase (i.e. biochar particle). Analysis of the EDS elemental maps suggested that nutrient elements, such as K and P, were also present within the mineral phases, possibly in the form of K_2SO_4 and phosphate precipitates ($Mg_3(PO_4)_2$/$FePO_4$), respectively. Other elements, such as Ca, Ti and Mn, were also noted within the mineral phases of the EB.

Cross-sectional TEM observations (Fig. 2) at the interface between the biochar and the adjacent mineral phases indicated that the attached mineral phases were in the form of very fine grains, typically a few 10's of nanometer in diameter. The microstructures of all three EBs studied were broadly similar irrespective of the torrefaction temperature applied or clay type added. The incorporation of biochar with clay and mineral phases is believed to contribute to both biochar stablization in soils and carbon sequestration (Nguyen et al., 2008; Lin et al., 2012c). Soil organic carbon occlusion within aggregates is one mechanism of carbon stabilization in soils (Jastrow et al., 2007).

XPS analysis, shown in Table 3, indicated that carboxylic groups were present in all three EBs. The presented XPS data is accurate to ±2% (relative). This supports the suggestion that reactions had occurred between the biochar particles and the mineral phases during torrefaction. It appeared that the torrefaction temperature did not generate significant differences with respect to the carbon bonding state. That is, similar data were acquired for EB-1 and EB-2. However, analysis of the nitrogen bonding state showed an increase in the concentration of N—C bonds in EB-2, relative to EB-1, implying more N has become incorporated into structures resistant to heating at the higher torrefaction temperature of 220 °C (in EB-2). When a coal tailings material (Clay-2) was used, i.e. for EB-3, both the carbon and nitrogen bonding states were found to have changed, compared to the other two EBs. The relative content of the C—O bonds increased in EB-3. It is quite possible that this arose from the organic carbon included in the

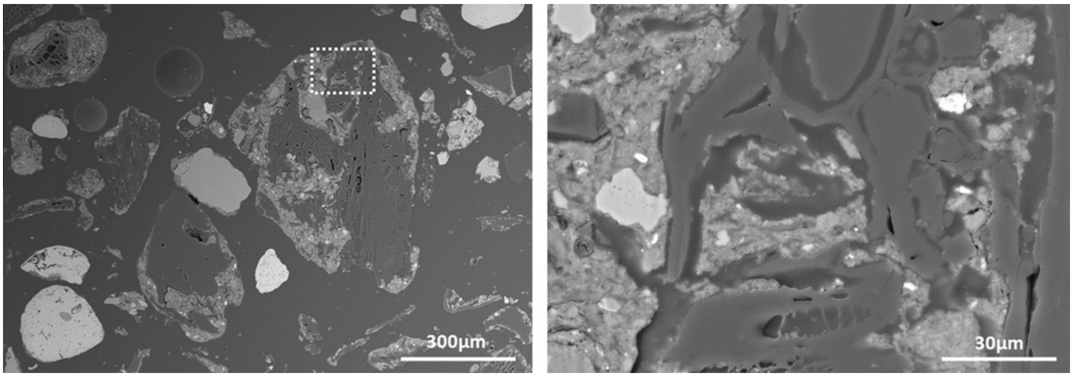

Fig. 1. Cross-sectional backscattered electron SEM images from an enhanced biochar (EB-1).

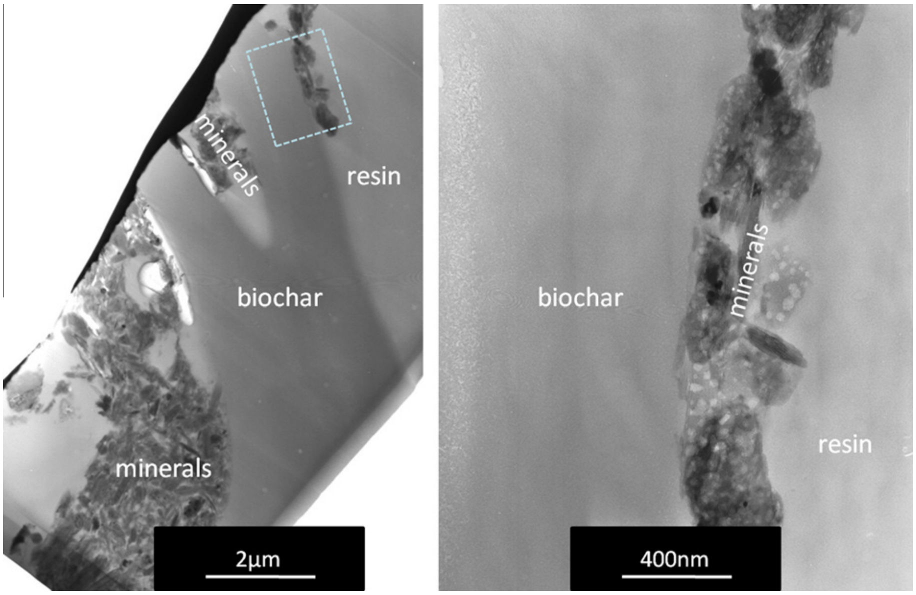

Fig. 2. Cross-sectional bright field TEM image across the interface between biochar and adjacent mineral phases (From EB-2).

Table 3
C 1s and N 1s bonding state and its relative atomic percentage (at.% ± 2% relative) on the EB surfaces as determined by XPS (N/D = non-detected).

Line	Binding energy (eV)	Structure	EB-1	EB-2	EB-3
C 1s	285	C—C/C—H	76	74	64
	286.5 ± 0.1	C—O	9	11	20
	288.1 ± 0.2	C═O	12	9	12
	289.2 ± 0.1	Carboxylic	4	6	4
N 1s	399.0 ± 0.1	N—C	15	25	19
	400.2 ± 0.2	Amino-acid N	85	75	71
	401.1 ± 0.2	Ammonium N	N/D	N/D	10

coal tailings used (see Table 1). Moreover, NH_4^+ was detectable in EB-3, but was hardly identified in the other two samples. This may have resulted from the N-containing compounds present in Clay-2, which contained 1.32% N. Alternatively, a relatively weaker interaction between the clay mineral and the biochar in EB-3 may have occurred because additional organic carbon was available from the coal tailings (mixtures of clay and biomass organic matter from washing the coal surfaces). This may subsequently left some active sites (such as carboxylic function groups) on the biochar surface which were able to absorb NH$_<$*ce* : *inf* > 3 < /*ce* : *inf* > /NH_4^+ (Iyobe et al., 2004; Asada et al., 2006), which could then present as plant available N in EB-3 (to be discussed).

DOC extracted from the EBs was measured by LC-OCD (Table 4). The results indicated that all the EBs contained a significant quantity of DOC, which presumably arose from the presence of CL (Tan et al., 1975), the partially decomposed organic matter in the CL, and dissociated DOC from the SIM biochar due to the H_3PO_4 treatment (Lin et al., 2012b). With the increase of torrefaction temperature from 180 (for EB-1) to 220 °C (for EB-2), the content of DOC increased, possibly resulting from greater decomposition occurring at the higher temperature. For EB-3, another possible source of DOC may have been the coal tailings material (Clay-2) used, due to the labile carbon contained (as shown in Table 1) and its transformation during torrefaction, which contributed to the highest DOC content in EB-3.

Further quantitative analysis on the fractions of DOC showed that, in comparison to that of the SIM biochar itself, more biopolymer, humic substances, building blocks and low molecular weight (LMW) neutrals were included in the EBs. However, a relatively lower content of LMW acids was noted. A hydrophobic fraction was detected in EB-1 and EB-2, but not in EB-3, possibly because the affinity (hydrophobicity) of Clay-1 used in the mixtures towards hydrophobic compounds is insufficient to absorb all such compounds generated during torrefaction. The measured humic substances fraction in the EBs possessed lower molecular weight, higher aromaticity and higher N/C ratio, with respect to that of the SIM biochar, which was probably caused by the adsorption of high molecular weight portion of humic substances onto clay (Balcke et al., 2002) and/or precipitation (Münch et al., 2002) due to the acidic condition (H_3PO_4 pre-treatment). The increase in N/C ratio of the humic substances was probably associated with alteration of N-containing compounds included in the decomposed CL organic matter and dissociated labile carbon matter, and resulted in the increase of hydrophilicity which weakened the affinity of aromatic humic substances towards the clays. As a result of this, this portion of humic substances remained soluble. The increase in building blocks and the LMW neutrals fraction possibly arose

Table 4
The concentration of DOC and its fractions (standard deviation ⩽2%) in the SIM biochar and BMs measured by LC-OCD.

	DOC	Hydrophobic DOC		Hydrophilic DOC												
				Biopolymer		Humics					Building blocks		LMW-neutrals		LMW-acids	
	ppb-C	ppb-C	%	ppb-C	%	ppb-C	%	N/C	Aromaticity	MW	ppb-C	%	ppb-C	%	ppb-C	%
SIM	3.63×10^3	n.q.	0.0	13	0.3	1.39×10^2	3.8	0.01	1.7	528	3.08×10^2	8.4	9.07×10^2	24.6	2.32×10^3	62.9
EB-1	6.55×10^4	4.72×10^3	7.2	3.87×10^3	5.9	3.12×10^4	47.7	0.06	4.3	357	1.41×10^4	21.5	1.15×10^4	17.6	1.15×10^2	0.2
EB-2	1.49×10^5	1.11×10^4	7.5	6.44×10^2	0.4	2.74×10^4	18.4	0.04	3.4	241	4.22×10^4	28.3	6.31×10^4	42.3	4.69×10^3	3.1
EB-3	1.92×10^5	n.q.	0.0	2.49×10^4	13.0	3.26×10^4	16.9	0.11	2.7	495	4.02×10^4	20.9	9.45×10^4	49.2	5	0.0

from the decomposition of both organic matter in CL and dissociated labile carbon during torrefaction. The decrease of LMW acids content is possibly due to the reactions of the LMW acids with both the clay and the added minerals.

With respect to the agricultural use of the EBs, elemental analysis results and some properties of the EBs are listed in Table 5. As can been seen, high concentrations of plant available P (Cowell P) and extractable ammonium-N were present in all the EBs. A high CEC and a high concentration of exchangeable K and Ca were noted in EB-1 and EB-2.

It was noted that the concentration of plant available P was proportional to the DOC concentration in all three EBs (linear relation, $R^2 = 0.986$), irrespective of the clay type used. (The total P content was similar in all three EBs). This was possibly because of the strong interactions between clay mineral phases and the high concentrations of DOC that were generated during torrefaction. In particular, humic substances and LMW acids are effective in blocking the P adsorption sites of clay and mineral phases, which resulted in a high concentration of plant available P (Haynes and Mokolobate, 2001). It has been reported (Gerke et al., 2000; Xu et al., 2012) that the addition of LMW organic acids and anions to soils can solubilise significant quantities of fixed P and maintain the P biologically available for most plants, with no significant effects on the concentrated HCl-extractable P and organic-P content (Xu et al., 2012). Moreover, Alvarez et al. (2004) stated that humic substances can influence the inorganic phosphate availability by inhibiting formation of thermodynamically stable calcium phosphate crystal phases, such as octa-calcium phosphate, which may modify the availability of these compounds in soils by changing the crystallisation behaviour from solution. In this study, the higher torrefaction temperature promoted the decomposition reactions of the CL organic matter and dissociated labile carbon from biochar, and produced a higher concentration of DOC. This higher concentration of DOC may solubilise mineral P and prohibit mineral P from adsorption onto clays or crystallization to thermodynamically stable phosphate crystal phases, this, therefore, may also contribute to the high content of plant available P.

Table 5
Elemental analysis and properties of the final products — EBs.

	Unit	Limit of reporting	EB-1	EB-2	EB-3
EC	Ds. m^{-1}	0.01	8.1	8.1	2.8
pH (CaCl2)	pH units	0.04	6.2	6.6	6.8
Colwell P	mg kg^{-1}	2	1600	2600	2900
Total nitrogen	%	0.02	1	1.3	0.84
Total carbon	%	0.2	36	30	42
KCl extractable ammonium-N	mg kg^{-1}	0.3	380	45	660
KCl extractable nitrate-N	mg kg^{-1}	0.2	120	<0.2	0.55
Acid neutralising capacity	%CaCO3	0.5	12	12	14
Ash elemental analysis					
Aluminium	%	0.0005	1.4	1.4	0.21
Arsenic	mg kg^{-1}	5	<5	<5	<5
Boron	mg kg^{-1}	4	10	11	15
Calcium	%	0.0003	6.3	6.8	6.8
Cadmium	mg kg^{-1}	0.3	4.5	4.7	<0.3
Cobalt	mg kg^{-1}	0.4	11	13	5.4
Chromium	mg kg^{-1}	0.2	19	23	10
Copper	mg kg^{-1}	0.2	52	35	30
Iron	%	0.00003	0.84	1.3	0.7
Potassium	%	0.0004	1.2	1.3	0.47
Magnesium	%	0.00006	0.17	0.25	1.4
Manganese	mg kg^{-1}	0.1	4100	5800	2100
Molybdenum	mg kg^{-1}	0.3	<0.3	<0.3	2.4
Sodium	%	0.0005	0.11	0.21	0.18
Nickel	mg kg^{-1}	0.7	10	12	6.4
Phosphorus	%	0.0003	2.9	2.9	2.6
Lead	mg kg^{-1}	2	6.1	6.8	4.5
Sulphur	%	0.0006	0.72	0.78	0.46
Selenium	mg kg^{-1}	4	<4	<4	<4
Zinc	mg kg^{-1}	0.8	150	120	130
Exchangeable cations					
Aluminium	cmol(+) kg^{-1}	0.01	0.25	0.17	<0.01
Calcium	cmol(+) kg^{-1}	0.01	20	22	10
Potassium	cmol(+) kg^{-1}	0.02	21	19	7.8
Magnesium	cmol(+) kg^{-1}	0.008	5.8	6.3	5.9
Sodium	cmol(+) kg^{-1}	0.02	3	5	3.7
CEC	cmol(+) kg^{-1}		50	52	27

For plant available N, it was noted that, although the total N content in EB-3 was lowest among the EBs, the highest NH_4^+ was found in this mixture, which was consistent with the XPS data (Table 3). Specifically that ~10 at.% of the total N was in the form of NH_4^+. This is possibly due to the higher nitrogen content contained in Clay-2 and strong interactions between DOC (the highest DOC content was in EB-3) and the clay and mineral phases, which left some active sites available on the biochar surface, so that NH_3/NH_4^+ could be absorbed (Iyobe et al., 2004; Asada et al., 2006) and preserved without any structural change. In contrast, the total N content was highest in EB-2, but the extractable N was the lowest, implying nitrogen transformation and combination with carbon, such as incorporation into the heterocyclic structures resistant to heating at moderate temperatures, which was also consistent with the XPS results that showed N in the N—C bonding state increased to ~25 at.% of the total N content. The incorporation of N has long-term consequences for N availability (Knicker and Skjemstad, 2000). It was reported by Jansen and van Bekkum (1995) that HNO_3 pre-oxidised activated carbon reacted with ammonia gas at 230 °C and the resultant material contained both lactam and imide functional groups. It was implied that, except for adsorption, ammonia could also react with biochar to form N-containing functional groups. The differences in N bonding state between EB-2 and EB-3 probably arose from Clay-2 (in EB-3), which included higher concentrations of N and S, as it has been found that S-containing groups enhanced ammonia adsorption (Petit et al., 2010).

Regarding to CEC and the content of exchangeable cations of K and Ca in the EBs (Table 5), it is likely dominated by the added clay type, and torrefaction temperature had little effect on the properties. As shown in Table 2, Clay-1 included more muscovite, which has a higher CEC than that of kaolinite (the principal component in Clay-2). Other micro-nutrients, such as Zn and Mn, were added through the mineral phases used, which may meet the need of some particular plants or soils (Fageria et al., 1997).

In this study, the highest amount of N conserved in the EBs was ~73% of the initial total N in EB-2, and the lowest was ~39% in EB-3. The interaction of biochar and ammonia produced from CL clearly plays an important role in N conservation. Strong adsorption of ammonia onto biochar surfaces could result in more N incorporation into the N—C bonding state within aromatic and/or heterocyclic structures, so that more N was preserved, which was then not immediately available to plants (as in EB-2). A high concentration of DOC may weaken the interaction between clay (as in EB-3) and biochar, and result in more NH_3/NH_4^+ adsorption, and subsequently more plant available N. It would be expected that higher biochar content might inhibit N losses in EB-3 during torrefaction. However, attention should be paid to the pH value change. As found in EB-3, the highest pH = 6.8 was noted, which may be an additional reason for its high N losses (Nahm, 2003), with respect to the other EBs.

4. Conclusions

Torrefaction of biochar mixed with CL, clay and minerals at moderate temperatures can result in biochar mixtures with high plant available nutrients and CEC. The highest N conservation was 73% of the initial total N in the feedstocks. Nitrogen incorporation into heterocyclic structures resulted in stable N-compounds, which has long-term consequences for N availability. The plant available P content was proportional to the concentration of DOC contained and generated during torrefaction of the EBs. It is believed that the high concentration of DOC in the EBs is contributed to the high content of plant available P. The CEC of the EBs is likely dominated by the clay type, rather than torrefaction temperature. The process used to generate these EBs conserved most of the plant nutrients in the CL, and generated biochar-clay/mineral aggregates with some micro-nutrients, such as Zn and Mn present. This provides a feasible way to efficiently utilise the nutrients present in CL and combine them with other nutrient element phases. These EBs have potential to be used as organic fertilizers or in soil amendment in sustainable agriculture.

Appendix A. Supplementary material

Supplementary data associated with this article can be found, in the online version, at http://dx.doi.org/10.1016/j.chemosphere.2012.11.063.

References

Alvarez, R., Evans, L.A., Milham, P.J., Wilson, M.A., 2004. Effects of humic material on the precipitation of calcium phosphate. Geoderma 118, 245–260.

Asada, T., Ohkubo, T., Kawata, K., Oikawa, K., 2006. Ammonia adsorption on bamboo charcoal with acid treatment. J. Health Sci. 52, 585–589.

Balcke, G.U., Kulikova, N.A., Hesse, S., Kopinke, F.-D., Perminova, I.V., Frimmel, F.H., 2002. Adsorption of humic substances onto kaolin clay related to their structural features. Soil Sci. Soc. Am. J. 66, 1805–1812.

Bernal, M.P., Alburquerque, J.A., Moral, R., 2009. Composting of animal manures and chemical criteria for compost maturity assessment. A review. Bioresour. Technol. 100, 5444–5453.

Cao, X., Harris, W., 2010. Properties of dairy-manure-derived biochar pertinent to its potential use in remediation. Bioresource Technol. 101, 5222–5228.

Chia, C.H., Munroe, P., Joseph, S.D., Lin, Y., Lehmann, J., Muller, D.A., Xin, H.L., Neves, E., 2012. Analytical electron microscopy of black carbon and microaggregated mineral matter in Amazonian dark earth. J. Microsc. 245, 129–139.

Clough, T.J., Condron, L.M., 2010. Biochar and the nitrogen cycle: introduction. J. Environ. Qual. 39, 1218–1223.

Fageria, N.K., Baligar, V.C., Jones, C.A., 1997. Field crops and mineral nutrition. In: Growth and Mineral Nutrition of Field Crops. Marcel Dekker, New York, pp. 1–10.

Faridullah, Yamamoto, S., Irshad, M., Uchiyama, T., Honna, T., 2008. Phosphorus fractionation in chicken and duck litter burned at different temperatures. Soil Sci. 173, 287–295.

Gaskin, J.W., Steiner, C., Harris, K., Das, K.C., Bibens, B., 2008. Effect of low-temperature pyrolysis conditions on biochar for agricultural use. Trans. ASABE 51, 2061–2069.

Gerke, J., Beißner, L., Römer, W., 2000. The quantitative effect of chemical phosphate mobilization by carboxylate anions on P uptake by a single root. I. The basic concept and determination of soil parameters. J. Plant Nutr. Soil Sci. 163, 207–212.

Glaser, B., Lehmann, J., Zech, W., 2002. Ameliorating physical and chemical properties of highly weathered soils in the tropics with charcoal: a review. Biol. Fert. Soils 35, 219–230.

Haynes, R.J., Mokolobate, M.S., 2001. Amelioration of Al toxicity and P deficiency in acid soils by additions of organic residues: a critical review of the phenomenon and the mechanisms involved. Nutr. Cycl. Agroecosys. 59, 47–63.

Huber, S.A., Balz, A., Abert, M., Pronk, W., 2011. Characterisation of aquatic humic and non-humic matter with size-exclusion chromatography – organic carbon detection – organic nitrogen detection (LC-OCD-OND). Water Res. 45, 879–885.

Iyobe, T., Asada, T., Kawata, K., Oikawa, K., 2004. Comparison of removal efficiencies for ammonia and amine gases between woody charcoal and activated carbon. J. Health Sci. 50, 148–153.

Jansen, R.J.J., van Bekkum, H., 1995. XPS of nitrogen-containing functional groups on activated carbon. Carbon 33, 1021–1027.

Jastrow, J.D., Amonette, J.E., Bailey, V.L., 2007. Mechanisms controlling soil carbon turnover and their potential application for enhancing carbon sequestration. Climatic Change 80, 5–23.

Jindo, K., Suto, K., Matsumoto, K., García, C., Sonoki, T., Sanchez-Monedero, M.A., 2012. Chemical and biochemical characterisation of biochar-blended compostsprepared from poultry manure. Bioresour. Technol. 110, 396–404.

Joseph, S., Camps-Arbestain, M., Lin, Y., Munroe, P., Chia, C.H., Hook, J., Van Zwieten, L., Kimber, S., Cowie, A., Singh, B.P., Lehmann, J., Foidl, N., Smernik, R.J., Amonette, J.E., 2010. An investigation into the reactions of biochar in soil. Aust. J. Soil Res. 48, 501–515.

Kithome, M., Paul, J.W., Bomke, A.A., 1999. Reducing nitrogen losses during simulated composting of poultry manure using adsorbents or chemical amendments. J. Environ. Qual. 28, 194–201.

Knicker, H., Skjemstad, J.O., 2000. Nature of organic carbon and nitrogen in physically protected organic matter of some Australian soils as revealed by solid state ^{13}C and ^{15}N NMR spectroscopy. Aust. J. Soil Res. 38, 113–127.

Liang, B., Lehmann, J., Solomon, D., Kinyangi, J., Grossman, J., O'Neill, B., Skjemstad, J.O., Thies, J., Luizão, F.J., Petersen, J., Neves, E.G., 2006. Black carbon increases cation exchange capacity in soils. Soil Sci. Soc. Am. J. 70, 1719–1730.

Lin, Y., Munroe, P., Joseph, S.D., Henderson, R., 2012a. Migration of dissolved organic carbon in biochars and biochar–mineral complexes. Braz. Agri. Res. 47, 677–686.

Lin, Y., Munroe, P., Joseph, S., Henderson, R., Ziolkowski, A., 2012b. Water extractable organic carbon in untreated and chemical treated biochars. Chemosphere 87, 151–157.

Lin, Y., Munroe, P., Joseph, S., Kimber, S., van Zwieten, L., 2012c. Nanoscale organo–mineral reactions of biochars in a ferrosol: an investigation using microscopy. Plant Soil. http://dx.doi.org/10.1007/s11104-012-1169-8.

Münch, J.-M., Totsche, K.U., Kaiser, K., 2002. Physicochemical factors controlling the release of dissolved organic carbon from columns of forest subsoils. Eur. J. Soil Sci. 53, 311–320.

Munroe, P., 2009. The application of focused ion beam microscopy in the material sciences. Mater. Charact. 60, 2–13.

Nahm, K.H., 2003. Evaluation of the nitrogen content in poultry manure. World Poultry Sci. J. 59, 77–88.

Nguyen, B.T., Lehmann, J., Kinyangi, J., Smernik, R., Riha, S.J., Engelhard, M.H., 2008. Long-term black carbon dynamics in cultivated soil. Biogeochemistry 89, 295–308.

Ogunwande, G.A., Osunade, J.A., Adekalu, K.O., Ogunjimi, L.A.O., 2008. Nitrogen loss in chicken litter compost as affected by carbon to nitrogen ratio and turning frequency. Bioresour. Technol. 99, 7495–7503.

Petit, C., Kante, K., Bandosz, T.J., 2010. The role of sulfur-containing groups in ammonia retention on activated carbons. Carbon 48, 654–667.

Shinogi, Y., Yoshida, H., Koizumi, T., Yamaoka, M., Saito, T., 2003. Basic characteristics of low temperature carbon products from waste sludge. Adv. Environ. Res. 7, 661–665.

Steiner, C., Das, K.C., Melear, N., Lakly, D., 2010. Reducing nitrogen loss during poultry litter composting using biochar. J. Environ. Qual. 39, 1236–1242.

Taghizadeh-Toosi, A., 2011. Ammonia and Nitrous Oxide Emissions from Soils Under Ruminant Urine Patches and the Effects of Biochar Amendment on These Emissions and Plant Nitrogen Uptake, PhD thesis. Lincoln University, New Zealand.

Tan, K.H., Mudgal, V.G., Leonard, R.A., 1975. Adsorption of poultry litter extracts by soil and clay. Environ. Sci. Technol. 9, 132–135.

van Zweiten, L., Kimber, S., Morris, S., Chan, K.Y., Downie, A., Rust, J., Joseph, S., Cowie, A., 2010. Effect of biochar from slow pyrolysis of papermill waste on agronomic performance and soil fertility. Plant Soil 327, 235–246.

Xu, G., Shao, H., Xu, R., Nie, Y., Pei, Y., Sun, Z., Blackwell, M.S.A., 2012. The role of root-released organic acids and anions in phosphorus transformations in a sandy loam soil from Yantai. China. Afr. J. Microbiol. Res. 6, 674–679.